Environmental Technology & Innovation 39 (2025) 104228

Contents lists available at ScienceDirect

Environmental Technology & Innovation

journal homepage: www.elsevier.com/locate/eti

Nature-based stormwater management for aquifer recharge: Exploring bioclogging-induced challenges

Yuhui Wu [a,b,c], Ying Lu [a,*], Zihan Yan [d], Min Shi [e], Qiandan Wang [f], Tao Lyu [g,**], Ruoyu Jia [a], Ling Huang [c], Zhiliang Chen [c], Jianyu Chen [c], Xiaoming Song [b], Yuesuo Yang [a]

[a] *Key Lab of Groundwater Resources and Environment (Jilin University), Ministry of Education, Changchun 130021, China*
[b] *Key Lab of Eco-restoration of Regional Contaminated Environment (Shenyang University), Ministry of Education, Shenyang 110000, China*
[c] *South China Institute of Environmental Sciences, MEE, Guangzhou 510535, China*
[d] *Key Laboratory of Surficial Geochemistry, Ministry of Education, Department of Hydrosciences, School of Earth Sciences and Engineering, Nanjing University, Nanjing 210023, China*
[e] *School of Environmental Science and Engineering, Southern University of Science and Technology, Shenzhen 518055, China*
[f] *Heilongjiang Provincial Water Conservancy and Hydroelectric Power Investigation, Design and Research Institute, Harbin 150080, China*
[g] *Faculty of Engineering and Applied Sciences Cranfield University, Bedfordshire MK43 0AL, UK*

ARTICLE INFO

Keywords:
Advanced stormwater management
Biological clogging
Groundwater recharge
Water reuse
Nature-based solutions (NbS)

ABSTRACT

Utilising excess urban stormwater to recharge groundwater can effectively mitigate the problems caused by the over-exploitation of subsurface environments while simultaneously making full use of valuable water resources. However, bioclogging can significantly reduce the efficiency of recharge projects in practical applications. This study is distinguished by its comprehensive consideration of unsaturated hydraulic conditions during stormwater recharge, which can influence microbial activities and the evolution of bioclogging, setting it apart from the predominant focus on saturated conditions in previous research. Microbial activity in the media became more vigorous under unsaturated conditions, and the cell volume decreased to 33–50 % of that under saturated conditions. Under unsaturated conditions, microbial EPS exhibited a curled morphology. At 60 % saturation, the contents of LB-EPS and polysaccharides increased by 141.23 and 187.47 μg/g sand, respectively, compared to saturated conditions. The reduction in saturation weakened microbial migration, promoted their deposition on the media surfaces, and reduced the non-uniformity of interlayer distribution. Simultaneously, unsaturated seepage conditions attenuated the effect of flow velocity (0.5–2 mL/min) changes on microbial migration and deposition. Bioclogging under unsaturated seepage conditions was governed by both EPS action and the EPS-bacterial interaction, with EPS secretion significantly influencing the degree of internal bioclogging development. This work contributes to a more comprehensive understanding of the bioclogging mechanisms under the unique hydrodynamic conditions of stormwater recharge, enabling more precise prevention and control of bioclogging during artificial stormwater recharge.

* Correspondence to: College of New Energy and Environment, Jilin University, Changchun 130021, China.
** Corresponding author.
E-mail addresses: luying819@jlu.edu.cn (Y. Lu), t.lyu@cranfield.ac.uk (T. Lyu).

https://doi.org/10.1016/j.eti.2025.104228
Received 26 February 2025; Received in revised form 22 April 2025; Accepted 23 April 2025
Available online 24 April 2025

1. Introduction

The escalating impacts of urbanisation and climate change have triggered environmental disasters such as extreme rainfall and frequent flooding, intensifying the urgent need for sustainable water management solutions (Lebon et al., 2023; Marazuela et al., 2022). Nature-based solutions (NbS), particularly natural flood management (NFM), have attracted significant attention and deployment for leveraging natural processes to mitigate flood risks while offering additional benefits such as improved water quality and ecosystem restoration (Badjana et al., 2023). With the efforts of such green infrastructure, including wetlands, rain gardens, and infiltration basins, nature-based stormwater management enables the capture, treatment, and infiltration of stormwater (Luthy et al., 2019; Moreno et al., 2023; Rathay et al., 2018; Xu et al., 2022). Such approaches not only alleviate flood risks but also facilitate aquifer recharge, addressing critical water resource challenges, particularly in water-stressed regions (Cui et al., 2023).

Despite their promising outcomes, stormwater infiltration through permeable green infrastructure faces a key challenge of media clogging, which can significantly reduce infiltration rates and stormwater management efficacy (Escalante, 2015). Amongst the physical, chemical, and biological clogging processes (Jeong et al., 2018), bioclogging is considered the most prominent after removing suspended matter from the stormwater, and is particularly difficult to control and remediate once established (Pavelic et al., 2011; Yang et al., 2021). Bioclogging in the permeable substrate primarily arises from excessive microbial growth and the extracellular polymeric substances (EPS) secreted by microorganisms (Abukhanafer et al., 2021; Li et al., 2021; Xia et al., 2020). During artificial recharge, biofilms can draw nutrients from the flowing water and create potential adsorption sites for dissolved substances by producing hydrophilic EPS (More et al., 2014). Concurrently, the production of EPS mucus matrix provides structural support for biofilms, which largely determines their overall structure (Zhao et al., 2015). These interactions are influenced by system design and flow dynamics, leading to distinctive bioclogging behaviours due to varying rates of EPS development (Mauclaire et al., 2004). Thus, understanding the composition and dynamics of bioclogging in porous media is crucial to support the successful implementation of nature-based stormwater management strategies.

Previous studies on bioclogging in stormwater artificial recharge have primarily been conducted under saturated flow conditions (Cui et al., 2023; Wang et al., 2023; Xia et al., 2018). Nevertheless, stormwater recharge exhibits different hydrological cycles (Lebon et al., 2023), resulting in discontinuous, unsaturated seepage conditions with alternating wet and dry phases. The infiltration profile comprises two types of infiltration flow zones that vary with depth: the water distribution zone (saturated zone) and the water conduction zone (unsaturated zone) (Fig. 1). The saturated zone is typically 3–5 cm deep (Darnault et al., 2004), with most of the infiltration area remaining in an unsaturated state (Morales et al., 2010). Consequently, microorganisms often grow and reproduce rapidly in the unsaturated infiltration zone during the recharge process (Greskowiak et al., 2005; Morales et al., 2010), which needs to be comprehensively assessed.

Compared to saturated systems, unsaturated porous media exhibit lower water content, greater shear forces, and distinct flow pathways. The moisture content decrease will limit nutrient diffusion to microorganisms (Cruz-Paredes et al., 2021), and Roberson and

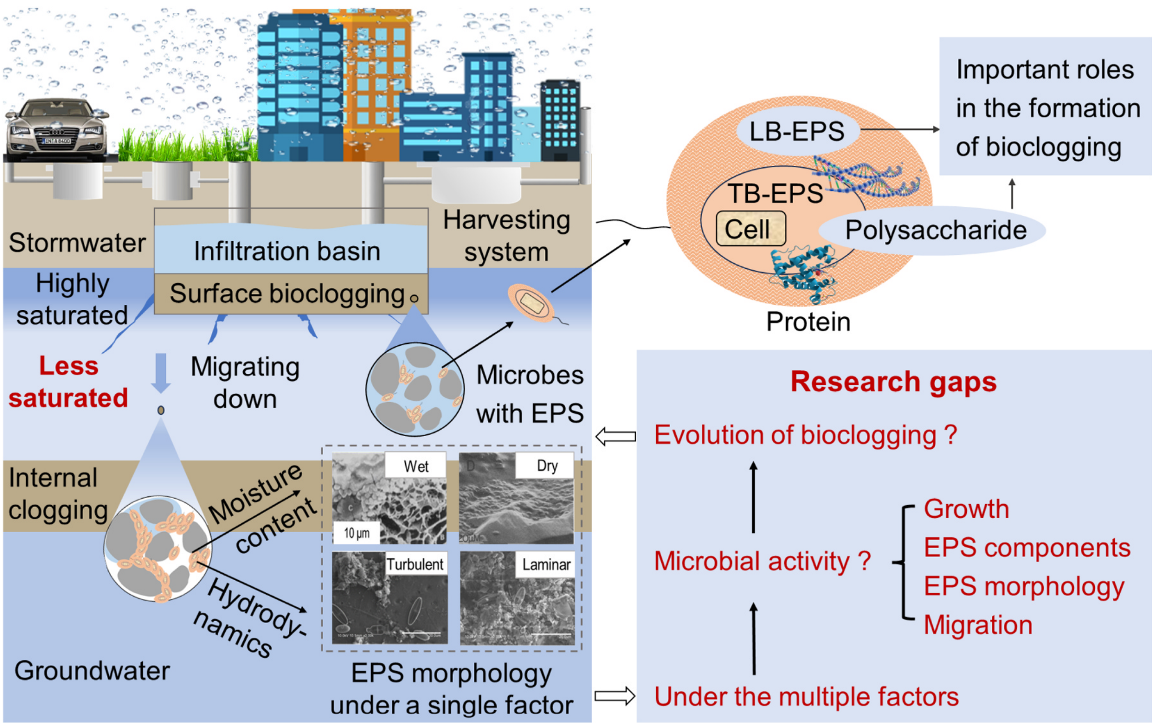

Fig. 1. Schematic diagram of bioclogging in stormwater artificial recharge.

Firestone (1992) have observed that the morphology of EPS changes with water content using electron microscopy. EPS appears soft and spongy under moist conditions but becomes hard and flattened when dry. The presence of EPS also enhances cell deposition in porous media (Tong et al., 2010). Microbial activities are also closely related to hydrodynamics in porous media (Ke et al., 2021). Previous studies have shown that higher shear forces can result in thinner and denser biofilms (Paul et al., 2012) and influence the composition and quantity of EPS secreted by microorganisms, promoting stable biofilm under specific water flow shear forces (Liu and Tay, 2002). On the other hand, increased shear forces can enhance biofilm detachment, allowing biofilms to travel through the media before redepositing in the pores, altering pore size and connectivity in deeper media layers. This idea is also considered as one of the main factors causing the reduction of the permeability coefficient of deep media (Metcalf, 2002). However, most studies on the response of microbial activity to changes in moisture content and water flow shear forces have only focused on the role of single factors (Pan et al., 2022; Shan et al., 2020; Wang et al., 2020b). The characteristics of microbial growth and the morphology and structure of EPS, as well as their migration and deposition characteristics, under the combined action of multiple factors under unsaturated seepage conditions are still unclear. The series of microbial metabolic processes inside the medium will further affect the formation and development of bioclogging in the me dium, which is the key constraint in the prevention and control of the stormwater bioclogging.

To address these knowledge gaps, this study aims to investigate the response of microorganisms and their EPS-induced bioclogging under the combined influences of unsaturated seepage characteristics during stormwater recharge (Fig. 1). The study evaluated the migration and deposition characteristics of microorganisms in porous media under unsaturated seepage conditions, as well as the role of flow velocity in this process. The changes of patterns in terms of morphology and composition of EPS secreted by microorganisms were also assessed. Moreover, the overall evolution process of bioclogging was also determined. The findings of this study provide new insights into the prevention and control of bioclogging in practical stormwater recharge engineering, enabling more efficient utilisation of stormwater resources.

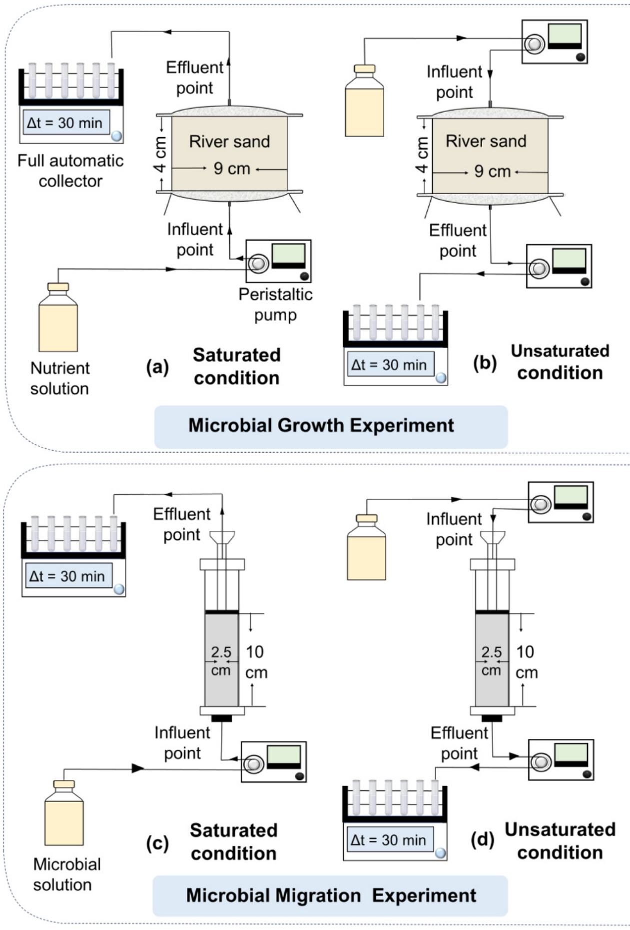

Experimental conditions for microbial growth

Number	Saturation degree	Run time (d)
G1	100%	8
G2	80%	8
G3	60%	8
G4	100%	14
G5	80%	14
G6	60%	14

Experimental conditions for microbial migration

Number	Saturation degree (%)	Flow rate (mL/min)
M1	100	1.0
M2	80	1.0
M3	60	1.0
M4	100	0.5
M5	60	0.5
M6	100	2.0
M7	60	2.0

Fig. 2. The experimental setup for microbial growth/migration and operating conditions.

2. Materials and methods

2.1. Experimental setup

To elucidate the mechanisms governing vertical stormwater infiltration during artificial recharge of the aquifer, two series of laboratory-scale column experiments were systematically conducted. The experimental setup primarily consisted of an organic simulation column, inlet solution, peristaltic pump, and fully automated collector (Fig. 2). The columns with a height of 4 cm and a diameter of 9 cm were used to assess microbial growth dynamics (Figs. 2a and 2b). For the microbial migration experiments, columns were designed with a height of 20 cm, an effective fill height of 10 cm during the experiments, and an internal diameter of 2.5 cm (Figs. 2c and 2d). 2). Considering that highly permeable zones are commonly targeted in artificial recharge engineering practices, this study adopted natural river sand with a particle size of 0.35–0.50 mm as the porous medium, following the lithological characteristics of the recharge formations reported by Zheng et al. (2014). The sand was sterilised by autoclaving at 121 °C for 30 minutes over three consecutive cycles, with a one-day interval between each cycle, to effectively remove native microorganisms and minimise interference with the experimental results (Süßmuth et al., 2024).

Three saturation levels (60 %, 80 %, and 100 %) were selected to represent a range of hydrological conditions from unsaturated to fully saturated states within the infiltration zone. A saturation level of 100 % reflects fully saturated conditions typically associated with continuous or high-intensity recharge events. In contrast, saturation levels of 60 % and 80 % represent moderately to weakly saturated states, which are more representative of conditions encountered during intermittent recharge or in highly permeable subsurface media. Preliminary trials and experimental observations revealed that maintaining a stable and controlled saturation level became increasingly challenging when the saturation dropped below 60 %, thus establishing the lower bound for the experimental design. Separate experiments were conducted to analyze microbial growth and migration in porous media under these varying degrees of saturation (Fig. 2). All experiments were performed at 25 °C.

2.2. Experimental operational conditions for microbial growth

2.2.1. Influent water preparation

The simulated stormwater solution was prepared by mixing tap water with appropriate nutrients (Xia et al., 2014). The nutrient solution consisted of 2.5 g/L glucose and 1.1 g/L potassium nitrate. Additionally, 1 mL of micro-nutrient element solution was added per litre, with the following specific components (unit: g/L): $FeSO_4 \cdot 7H_2O$ (0.01), $CuSO_4 \cdot 5H_2O$ (0.01), $MnSO_4 \cdot 6H_2O$ (0.02), $ZnSO_4 \cdot 7H_2O$ (0.025), $Na_2MoO_4 \cdot 2H_2O$ (0.01), $NaSeO_4 \cdot 2H_2O$ (0.01), $CoCl_2 \cdot 6H_2O$ (0.05), $NiCl_2 \cdot 6H_2O$ (0.01). The pH of the nutrient solution was adjusted to 7.0 and sterilised by autoclaving at 121 °C for 30 minutes.

2.2.2. Preparation of bacterial solution

To accelerate the stabilisation of the newly established infiltration system, *Pseudomonas aeruginosa*, a commonly used model microorganism in the study of artificial recharge bioclogging (Cui et al., 2021b; Ye et al., 2022), was introduced into the system. This strain was obtained from the China General Microbial Strain Preservation and Management Centre (CGMCC 1.10452, original number: GIM32) and inoculated into Luria-Bertani (LB) sterile liquid medium. The culture was incubated under constant temperature and agitation for 24 hours (30 °C, 120 rpm). The bacterial solution was then centrifuged at 8000 rpm for 5 minutes, and the cells were washed three times with PBS solution. The optical density of the bacterial suspension was adjusted to $OD_{600} = 1.0$ using PBS.

2.2.3. Operation of the columns

The sand was packed into the columns using the wet method with the bacterial suspension, resulting in an initial porosity of 0.37. The sand columns were then left to stand for 4 hours to allow stable adhesion of the model microorganisms to the media. The saturated group was directly fed with nutrient solution from the bottom to the top. In the unsaturated groups, the target saturation levels were adjusted using a drainage method. After the column was fully saturated, a defined volume of solution was extracted from the bottom using a peristaltic pump to ensure that the remaining pore water corresponded to 80 % and 60 % of full saturation, respectively. Subsequently, influent solution was supplied from the top while effluent was simultaneously withdrawn from the bottom. By fine-tuning the relative flow rates of the influent and effluent peristaltic pumps, the internal saturation level of the column was stably maintained throughout the entire experiment. The procedure was adapted from the method described by Gargiulo et al. (2007). After the setup was completed, the unsaturated group was supplied with nutrient solution from the top to the bottom. Two recharge periods were established: columns G1–G3 were recharged for 8 days, while columns G4–G6 were recharged for 14 days (Fig. 2). The automatic sampling interval was set to 30 minutes. After the experiment, the media in the column were sampled layer by layer at one-centimetre intervals to determine changes in organic matter content. Simultaneously, the EPS on the sand surface was extracted and analysed, while microbial growth and EPS morphology were characterised and examined.

2.3. Procedures of microbial migration

According to the measured chemical properties of stormwater and the water quality standards for stormwater recharge, a 5 mM $NaHCO_3$ solution was selected as the background solution, with its pH adjusted to 7.5 for the experiment. Different saturation degrees (60 %, 80 %, 100 %) and flow rates (0.5, 1.0, 2.0 mL/min) were set in the experiments (Fig. 2). The flow rates were specifically designed to simulate rainfall-controlled infiltration rates of approximately 1.5, 3.0, and 6.0 m/day within the column. These hydraulic conditions were selected to match both the seepage characteristics of the chosen river sand particle size and the established experimental parameters employed in previous studies investigating clogging phenomena during artificial aquifer recharge (Cui et al., 2021a, Ramazanpour Esfahani et al., 2020). These hydraulic conditions were selected to match both the seepage characteristics of the chosen river sand particle size and the established experimental parameters employed in previous studies investigating clogging phenomena during artificial aquifer recharge (Cui et al., 2021a, Ramazanpour Esfahani et al., 2020). The pretreatment of the bacterial solution was consistent with the method described in Section 2.2.2.

The supplied bacterial solution was adjusted to an OD_{600} of 0.5 with the corresponding background solution of each group for the relevant experiments and changed every 2 hours to minimize the interference of bacterial sedimentation on the results of experiments.

The columns were filled by dry method with a bulk density of 1.67 g/cm^3. The peristaltic pump slowly supplied the background solution from the bottom up for 12 hours and the pore volume (PV) was 17 mL. The unsaturation adjustment of columns was the same as the growth group experiments. Subsequently, 1.5 mM NaCl solution (238 mL, 14PV) was injected into the column for the tracer experiment, and samples were collected at intervals of 0.25 PV to determine the Cl^- concentration. At the end of the rinsing of the tracer experiment, bacterial solution (357 mL, 21 PV) was supplied to each column, and then switched to $NaHCO_3$ solution (374 mL, 22 PV) under the conditions of the corresponding experimental group for rinsing. The effluent was collected by the automatic collector, with samples taken at intervals of 0.5 PV to determine the microbial content. After the experiment, the columns were sampled in layers by centimeter to measure the organic matter content on the surface of the media.

2.4. Analytical methods

2.4.1. Measurement of effluent parameters and media characterization analysis

The OD_{600} values were determined using a UV spectrophotometer (UV-1900i, SHIMADZU, Japan). Chloride concentrations were quantified with an ion chromatograph (930 Compact IC Flex, Metrohm, Switzerland). Organic matter content was assessed using the loss on ignition method (Farmer et al., 2014). The morphology of biofilms and EPS on the sand surface from the growth column experiments was characterised and analysed using scanning electron microscopy (JSM-6700F, JEOL, Japan).

2.4.2. Extraction and quantification of polysaccharides and proteins in EPS

The formaldehyde-NaOH method, recognised for its efficacy in EPS extraction (Hong et al., 2017; Liu and Fang, 2002), was chosen for this purpose (Fig. S1). The procedure followed Xia et al. (2014), with slight modifications. Protein quantification was conducted using an improved Folin-phenol method, with bovine serum albumin as the standard (Shen et al., 2013). Polysaccharide analysis employed the anthrone-sulphuric acid colourimetric method, with glucose as the standard (Wei et al., 2019). The total quantities of LB-EPS and TB-EPS were calculated as the sum of their respective protein and polysaccharide components, with the overall EPS content encompassing the combined LB-EPS and TB-EPS.

3. Results and discussion

3.1. Pattern of microbial growth under different saturation conditions

During the initial 90 minutes of operation, a significant bacterial concentration (OD_{600} up to 0.42) was observed in the effluent

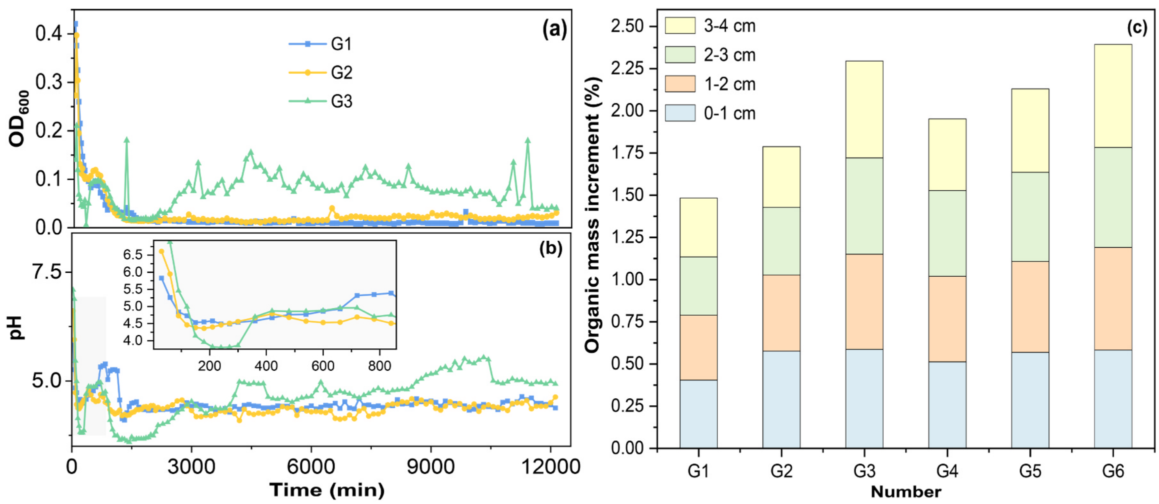

Fig. 3. Microbial growth in columns under different saturation conditions: (a) OD600 changes of effluent from columns; (b) pH changes of effluent from columns; (c) Change of organic matter content in each layer of column. G1–G3 represent groups with saturation levels of 100 %, 80 %, and 60 %, respectively, under 8-day recharge; G4–G6 represent corresponding saturation levels under 16-day recharge.

(Fig. 3a), which can be attributed to the washout of unestablished microbial strains with the influent water. The microbial community in the media appeared to have stabilized and adhered to the sand particles, leading to a noticeable reduction in bacterial concentration in the effluent after 300 minutes (Fig. 3a). Notably, differential stabilization patterns emerged among the experimental columns. As microbial growth entered the stabilization phase, the OD_{600} values in the effluents of columns G1 and G2 stabilized at lower levels, whereas column G3 exhibited continued dynamic fluctuations. The rapid decline in effluent pH from 7.0 to 4.5 (Fig. 3b) could be attributed to microbial metabolism under unsaturated conditions, where the nutrient solution with an initial pH of 7.0 (Section 2.2) likely underwent acidification due to the production of organic acids and other metabolic by-products.

Changes in organic matter content, primarily driven by microbial growth and reproduction in this study, served as a key indicator of microbial enrichment within the columns (Fig. 3c). Reducing saturation levels at the same recharge time significantly increased the organic matter content in each layer. Furthermore, the organic matter content in all columns exhibited a significant increase with prolonged recharge time. Notably, the difference in organic matter accumulation between saturated and unsaturated conditions diminished as the recharge time increased.

Due to prior extraction treatments applied to the unsaturated group, the initial bacterial solution volume in the columns at the same recharge time followed the order: G1 > G2 > G3. Calculations of the bacterial content in the effluent, based on data from Fig. 3a, revealed the following trend: effluent bacterial content was highest in G3, followed by G2 and G1 (G3 > G2 > G1). However, as illustrated in Fig. 3c, the increase in organic matter content followed a similar trend: G3 > G2 > G1. These findings indicate that microbial activity was more vigorous under unsaturated conditions, and that the intensity of this activity increased as saturation levels decreased.

3.2. Responses of microbial EPS and cell morphology

After the experiment, the sand from the surface layer (0–1 cm) and the middle layer (2–3 cm) of each column was analyzed using SEM (Fig. 4). To address potential heterogeneity in the distribution of unsaturation within the media, samples from the unsaturated columns were collected separately from both central and peripheral regions, thereby minimizing data variability and enhancing the reliability of the results.

The morphology of biofilms and EPS on the column media varied significantly with decreasing saturation at the same recharge time. After 8 days, the G1 column surface exhibited ripple structures under water flow shear (Fig. 4a), with EPS appearing smooth, flat, and densely packed, featuring localized small pores. As saturation decreased, these ripple patterns disappeared and EPS adopted a curled morphology (Figs. 4b and 4c). At 60 % saturation, G3 displayed curled EPS bands (Fig. 4d) and a fibrous three-dimensional network formed by intertwined bacteria and EPS in certain regions (Fig. 4e). These morphological adaptations were likely driven by decreased moisture availability and increased shear forces. In response, microorganisms contracted and curled the reticular EPS structure, slowing the drying of embedded bacterial cells, prolonging metabolic regulation, and enhancing survival (Flemming and Wingender, 2010; Or et al., 2007). Additionally, biofilms mitigated elevated shear stress through irreversible deformation and

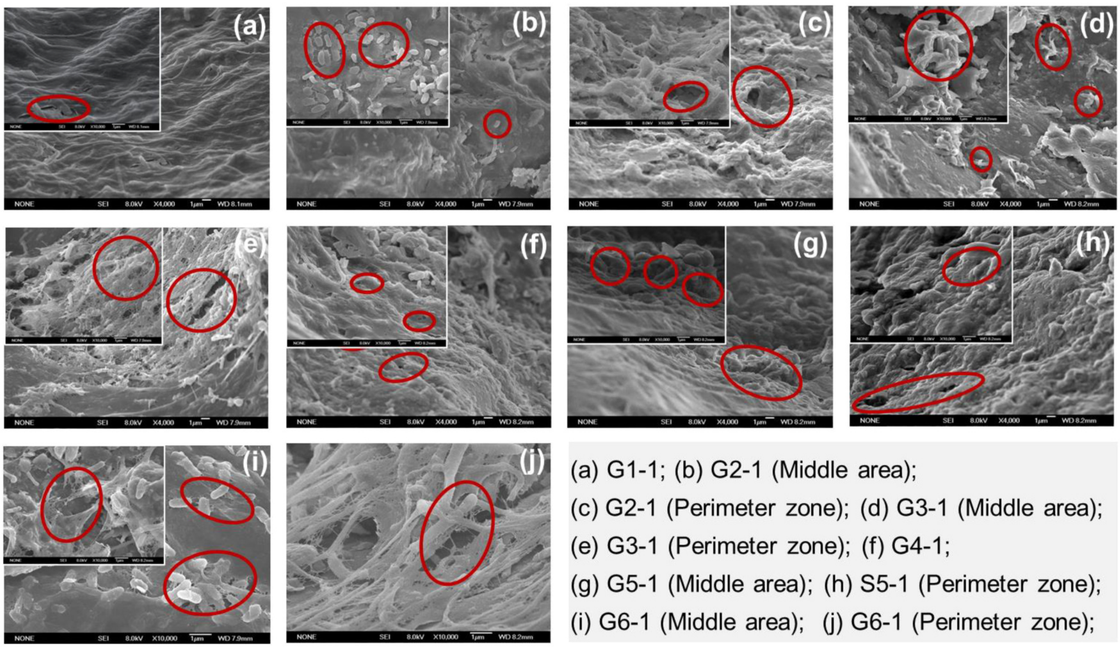

Fig. 4. SEM images of the surface layer (0–1 cm) sand from different groups after recharge: (1) G1–G3 represent groups with saturation levels of 100 %, 80 %, and 60 %, respectively, under 8-day recharge; (2) G4–G6 represent corresponding saturation levels under 16-day recharge.

structural rearrangement (Pechaud et al., 2024).

Biofilm thickness on the column surfaces increased significantly with extended recharge time. However, the effects of recharge time on EPS morphology and biofilm distribution varied with saturation levels. Under saturated conditions, EPS morphology on the media surface remained largely unchanged with increasing recharge time (Fig. 4f). In contrast, as saturation decreased, EPS distribution became increasingly heterogeneous. In the G5 column, large pores formed by curled EPS were evident, with some areas exhibiting distinct mucus-like stripes (Figs. 4g and 4h). Similarly, in the G6 column, bacterial cells were enveloped by EPS films characterized by numerous small surface pores (Fig. 4i) and a branching pattern (Fig. 4j).

EPS morphology also varied with distance from the inlet. At 2–3 cm from the inlet of the G1 column, biofilm thickness was reduced compared to the surface layer, with abundant bacterial cells visible in SEM images. EPS appeared as flat or banded films with smooth surfaces (Fig. S2). Under unsaturated conditions, biofilm and EPS distribution within the media was highly heterogeneous, with localized aggregation observed in some areas (Fig. S2).

EPS morphology under different saturation conditions significantly influenced nutrient transport within the media, thereby affecting microbial growth. In saturated columns, surface biofilms were smoother, with fewer and smaller EPS pores, which hindered nutrient migration and led to surface biomass accumulation. In contrast, under unsaturated conditions, curled EPS and larger pores facilitated nutrient transport inward. Additionally, increased shear forces caused biofilm detachment, enhancing internal biomass as biofilms migrated with water flow. This explained the higher internal biomass observed in unsaturated columns (Fig. 3c).

In addition, bacterial cells continuously altered their morphology to adapt to unsaturated conditions. Based on SEM images (Fig. 4), the estimated sizes of bacterial cells in the surface layer were 2.2–2.83 μm for G1, 0.91–1.82 μm for G2, and 0.93–1.09 μm for G3. These findings align with previous studies, such as Lin et al. (2014), which demonstrated that microorganisms can resist adverse environmental conditions by reducing their cell volume. When saturation decreased to 80 %, bacterial cell size was reduced by 45.72 % compared to saturated conditions. A further reduction in saturation from 80 % to 60 % resulted in a smaller decrease of 14.12 %,

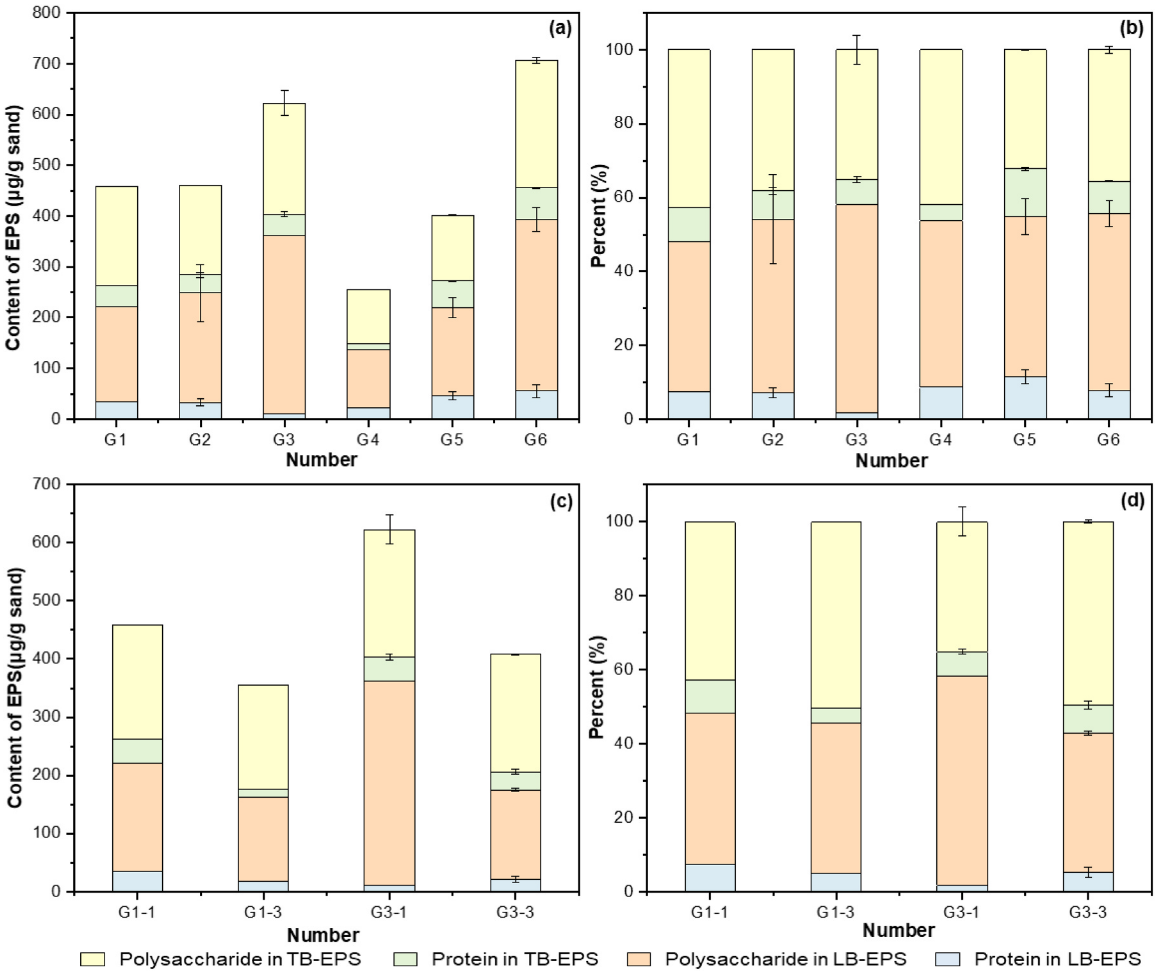

Fig. 5. Component content and proportion of EPS in sand column under different saturation conditions: (1) G1–G3 represent groups with saturation levels of 100 %, 80 %, and 60 %, respectively, under 8-day recharge; (2) G4–G6 represent corresponding saturation levels under 16-day recharge; (3) G1–1 and G3–1 refer to the surface layer (0–1 cm) near the inlet; (4) G1–3 and G3–3 refer to the layer 2–3 cm away from the inlet.

suggesting that the influence of decreasing saturation on bacterial morphology diminished once saturation dropped below 80 %.

3.3. Characterization of the EPS

3.3.1. EPS content and composition under different saturation levels

Microorganisms adapt to environmental changes by modulating the composition and content of EPS (Lin et al., 2014). After 8 days of recharge, surface EPS content increased by 164.17 μg/g sand as saturation decreased from 100 % (G1) to 60 % (G3) (Fig. 5a). This increase in EPS production was a stress response, enhancing the structural integrity of biofilms (Flemming and Wingender, 2010; Jara et al., 2020). Additionally, EPS created a protective microenvironment for microbial cells, retaining moisture and slowing the drying rate under reduced environmental water availability (Or et al., 2007). Thus, under decreasing saturation, microorganisms increased EPS secretion as a defensive adaptation.

The content of LB-EPS increased by 141.23 μg/g sand in G3 columns compared to G1, significantly higher than the increase in TB-EPS (22.94 μg/g sand) (Fig. 5a). This suggested that microorganisms preferentially secreted more LB-EPS under unsaturated conditions, consistent with findings by Ye et al. (2011) that unfavorable conditions stimulated LB-EPS production.

From a compositional perspective, microorganisms responded to unsaturated conditions by reducing protein secretion and increasing polysaccharide content (Fig. 5b). As the saturation decreased from saturated to 60 %, the polysaccharide content in LB-EPS increased by 164.62 μg/g sand, while the polysaccharide content in TB-EPS increased by 22.85 μg/g sand. At the same time, the protein content in LB-EPS decreased by 23.38 μg/g sand, with no significant change in protein content in TB-EPS. Since polysaccharides possess higher hygroscopicity and greater adhesive properties compared to proteins (Harimawan and Ting, 2016; Manzanera, 2021), their increased presence likely contributed to enhanced microbial survival and adaptability in unsaturated environments.

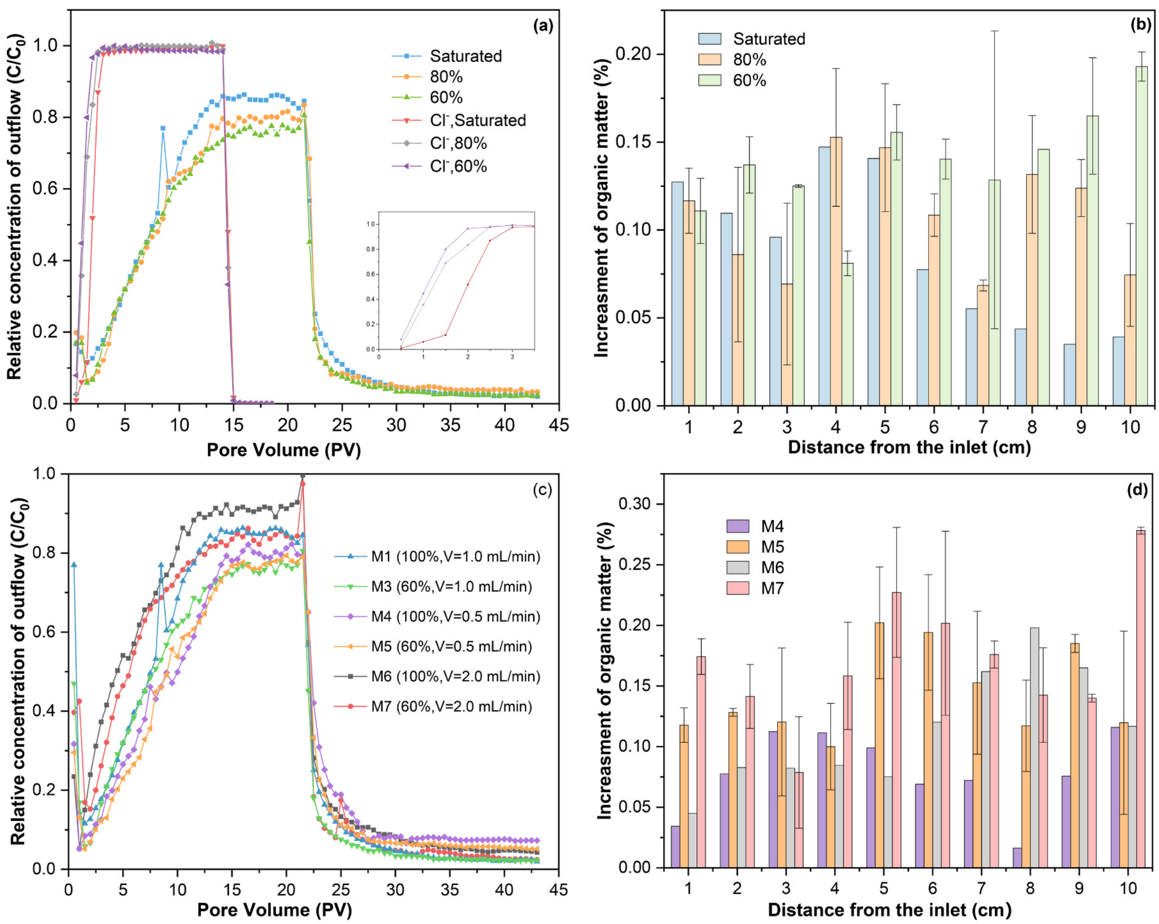

Fig. 6. Characteristics of microbial migration and deposition in columns: (a) Breakthrough curves of Cl$^-$ and microbial under different saturation conditions; (b) Deposition of microbial from the inlet to outlet under different saturation conditions; (c) Breakthrough curves of microbial under different flow rates; (d) Deposition of microbial from the inlet to outlet under different flow rates.

3.3.2. Spatial and temporal variations in EPS secretion

The influence of internal water content and flow shear force on EPS secretion was less pronounced in the interior layers compared to the surface (Figs. 5c and 5d). In all columns, surface EPS content was higher than that in the interior, where microbial metabolic activity was more pronounced due to the abundance of nutrients and oxygen near the inlet. Although the total EPS content in the interior of G3 was slightly higher than in G1, the difference was minimal.

As recharge time increased from 8 to 14 days, microorganisms adapted to the environment, entering a stable growth phase. EPS secretion gradually declined toward a stable level, with EPS content decreasing in most columns (except for a slight increase in G6). In the G5 column, total protein content in surface EPS increased by 43.2 % compared to G2, while in G6, it increased by 125.6 %. Proteins played a critical role in maintaining cellular structural integrity and stability (More et al., 2014). As microorganisms adapted to unsaturated conditions, they reallocated energy from polysaccharide synthesis to protein production, facilitating stable growth.

3.3.3. Implications for bioclogging

Previous studies indicated that polysaccharides were the primary contributors to bioclogging (Wang et al., 2020a), with the heightened LB-EPS content identified through structural analysis being the primary cause (Xia et al., 2016). Consequently, microbial activity on the surface under unsaturated conditions intensified, resulting in elevated EPS secretion, including higher levels of LB-EPS and polysaccharides, rendering it more susceptible to bioclogging.

3.4. Microbial migration and deposition under different saturation conditions

Based on the tracer experiment described in Section 2.3, the Cl^- breakthrough curves provide insights into solute transport behavior under different flow conditions. Reductions in saturation levels did not significantly affect the maximum effluent concentration of Cl^- during penetration but advanced the time to reach equilibrium (Fig. 6a). Notably, a decline in saturation from 100 % to 80 % corresponded to an advancement in penetration time from 2 pore volumes (PV) to 1.5 PV, whereas a subsequent decrease from 80 % to 60 % only yielded a marginal advancement of 0.25 PV. This indicated that once saturation decreased to 80 %, further reductions had a diminishing influence on Cl^- penetration.

Initially, substances on the sand surface migrated with the water flow, causing errors in the measured microbial concentration, which diminished after 2 PV (Fig. 6a). Following microbial liquid injection, the C/C_0 values in the effluent under different saturation levels increased rapidly. As more microbial cells occupied surface adsorption sites, the adsorption rate decreased notably, resulting in a slow increase in bacterial concentration in the effluent. After 21 PV, a sterile background solution was injected, causing a slight increase in bacterial counts in the effluent before a rapid decrease. This phenomenon could be attributed to the detachment of loosely attached bacterial cells under the shear force of water flow during flushing, followed by aggregation during outflow. In the later stages, effluent concentrations under all saturation levels were extremely low, approaching zero, with no tailing observed.

Reducing saturation delayed the time for microbial penetration to reach the plateau phase and decreased the maximum effluent ratio. When saturation was reduced to 60 %, the time to reach the plateau phase was extended by 2 PV, and the maximum efflux ratio dropped from 0.86 to 0.75. Similar conclusions were reported by Gargiulo et al. (2007) and Bai et al. (2017). Integral calculations of the penetration curves (Fig. 6a) were conducted to determine total microbial retention during the injection phase and total microbial efflux during the flushing phase (Table S1). In contrast to saturated conditions, an air-liquid interface existed under unsaturated conditions. Bacteria exhibited a greater affinity for the air-liquid interface than for the solid interface (Cui et al., 2021a), making them more inclined to attach to the air-liquid interface (Flury and Aramrak, 2017). Therefore, under unsaturated conditions, bacteria were more likely to attach to the surface of the media and remained more firmly attached after adhesion.

Under unsaturated conditions, the deposition of microbes did not exhibit a monotonic decrease in distribution characteristics (Fig. 6b). Moreover, the non-uniformity of microbial distribution within the column decreased as the saturation decreased. Microbial deposition was concentrated in the surface layer of 0–5 cm, with a certain monotonic decrease in the range of 5–10 cm as depth increased, but with a relatively small decrease in magnitude under saturated conditions. As the saturation decreased from 80 % to 60 %, the proportion of microbial deposition within the 0–5 cm depth range dropped from 50.92 % to 44.10 % of the total deposition. Gas-liquid interfaces existed in unsaturated media, and these interfaces were mobile boundaries, where colloids attached to it through capillary action could move freely under the influence of shear forces from water flow, Brownian motion, or surface tension (Aramrak et al., 2014; Lazouskaya et al., 2011). Therefore, microorganisms attached to the gas-liquid interface within an unsaturated porous media were further migrated and deposited by water flow.

Therefore, under the same recharge conditions, the presence of gas-liquid interfaces in unsaturated media significantly inhibited bacterial migration and promoted bacterial deposition, increasing the likelihood of internal bioclogging. However, the inhibitory effect of unsaturated conditions on bacterial migration did not continue to increase with further reductions in saturation. Once unsaturation reached 80 %, further reductions had a diminished influence on bacterial migration.

3.5. Microbial migration and deposition under different flow rates

Increasing the flow rate significantly enhanced microbial transport through porous media and reduced overall deposition (Fig. 6c, Table S2). At low flow rates (0.5 mL/min), microbial migration showed no significant difference between saturated and unsaturated conditions. However, as the flow rate increased, its effect became more pronounced under saturated conditions. When the flow rate increased from 0.5 mL/min to 1 mL/min, the time to reach the plateau phase under saturated conditions decreased by 2 PV, and the C/C_0 value increased by 0.05. In contrast, microbial penetration under unsaturated conditions showed no significant change. As the flow rate further increased to 2 mL/min, the time to reach the plateau phase under saturated conditions decreased by 4 PV, and the C/C_0 value increased to 0.91. Under unsaturated conditions, the time to reach the plateau phase shortened by 3 PV, with the C/C_0 value rising from 0.77 to 0.86. In unsaturated media, capillary forces at the gas-liquid interface caused some water to flow into smaller pores, creating low-speed zones (Sen, 2011; Torkzaban et al., 2006). Within this range, changes in flow rate had minimal impact on colloid migration. Since microorganisms were a type of biological colloid, flow rate changes within a certain range under unsaturated conditions reduced the influence of flow rate on microbial migration.

Overall microbial deposition decreased with increasing flow rates, but deposition unevenness became more pronounced (Fig. 6d). The impact of flow rate on microbial distribution was more significant under saturated conditions. When the flow rate increased from 0.5 mL/min to 2 mL/min, the proportion of deposition in the 0–5 cm surface layer of saturated columns increased by 22.7 %, compared to only 1.12 % in the 60 % saturation column. This suggested that unsaturated conditions significantly dampened the effect of flow rate on microbial deposition patterns.

3.6. *Influence of seepage state on the evolution of bioclogging*

The seepage state significantly influences microbial growth, EPS secretion, and the migration and deposition of microorganisms in porous media, thereby governing the evolution of bioclogging during artificial stormwater recharge, as illustrated in Fig. 7.

Our previous studies have demonstrated that under saturated seepage conditions, bioclogging in porous media progresses through three distinct stages: (1) the bacterial action stage, (2) the bacterial and EPS co-action stage, and (3) the EPS-dominated stage (Wang et al., 2022). However, during stormwater artificial recharge, the low nutrient content of stormwater created a nutrient-poor environment, which suppressed microbial activity (Fig. S3 and S4). This study revealed that under unsaturated seepage conditions, microorganisms adapted by reducing their cell volume and rapidly secreting large quantities of LB-EPS and polysaccharides (Fig. 7b). Both LB-EPS and polysaccharides have been widely recognized as critical contributors to bioclogging formation (Xia et al., 2016). Consequently, the initial phase of bioclogging was primarily driven by the massive secretion of EPS by microorganisms.

As the recharge process continued, microorganisms gradually adapted to unsaturated seepage conditions. During this phase, the proportion of LB-EPS and the polysaccharide content in the secreted EPS decreased, while the total EPS content exhibited a slight

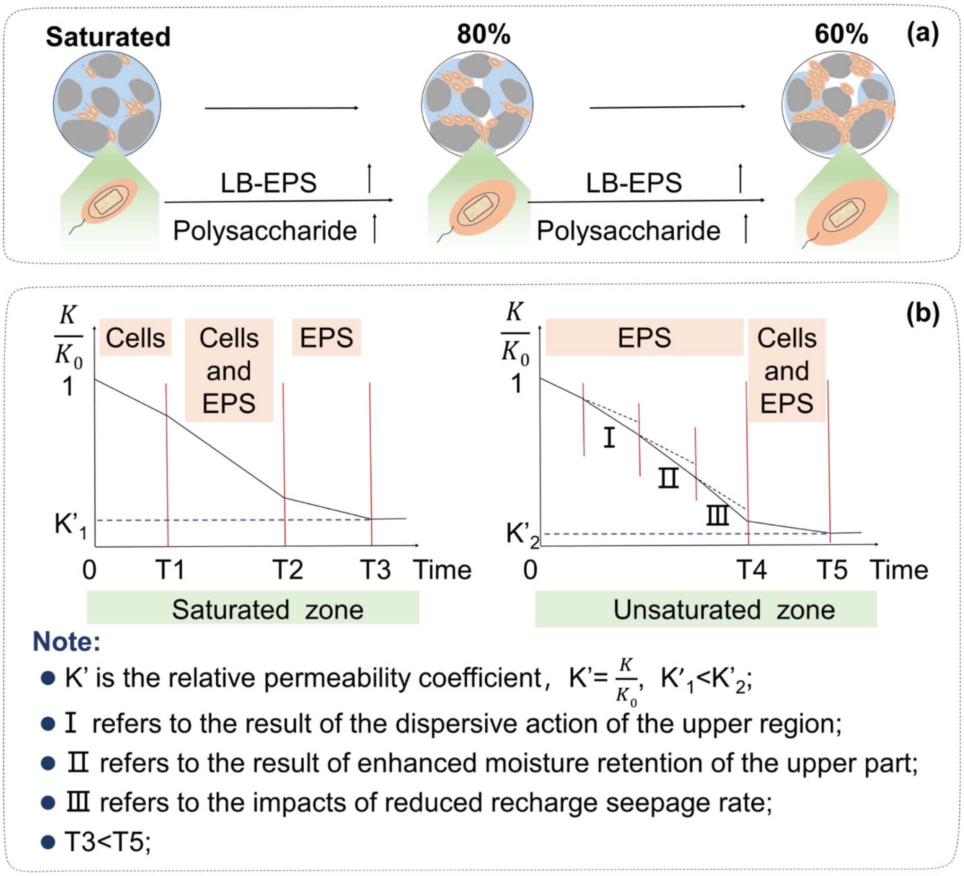

Fig. 7. Evolution process of bioclogging in stormwater artificial recharge:(a) Response of EPS content to saturation reduction; (b) Development of bioclogging within the media under different saturation conditions.

increase. At this point, bioclogging within the media was predominantly governed by the combined action of bacteria and EPS. Therefore, under unsaturated conditions during stormwater artificial recharge, bioclogging can be categorized into two stages: (1) the EPS-dominated stage and (2) the bacterial and EPS co-action stage (Fig. 7b).

The development of bioclogging under unsaturated seepage conditions is depicted in Fig. 7b. The secretion of EPS enhanced the moisture retention capacity of the media, shifting solute transport mechanisms toward diffusion-dominated processes (Wang et al., 2022). As the biofilm in the surface layer matured, some bacteria detached and migrated deeper into the media, facilitated by water flow and enhanced diffusion. This migration led to a further reduction in the internal permeability coefficient. Simultaneously, the unsaturated seepage conditions stimulated microorganisms to secrete additional EPS, rapidly increasing the moisture retention capacity in the affected regions. This exacerbated the uneven distribution of moisture near the surface layer, intensifying the unsaturated state in the lower regions and creating a positive feedback loop that promoted further EPS secretion and bioclogging. Moreover, a decrease in the seepage rate of recharge water caused bacterial aggregation in specific zones, further aggravating bioclogging.

In practical engineering applications, several management strategies can be derived from the findings of this study. For infiltration facility design, the incorporation of the establishment of oxidation zones in critical areas may effectively mitigate the synergistic clogging effects between extracellular polymeric substances (EPS) and bacteria under unsaturated conditions. Regarding operational management, dynamic adjustment of recharge strategies in response to seasonal variations is advised. For instance, dynamic saturation control combined with intermittent saturated flushing can promote the periodic removal of accumulated EPS, thereby achieving a balance between recharge efficiency and bioclogging mitigation.

4. Conclusion

This study investigated the effects of variable seepage conditions on microbial growth, migration, and EPS secretion, as well as the evolution of bioclogging during urban stormwater artificial recharge. The findings highlight significant differences in microbial behavior and bioclogging development under saturated and unsaturated conditions. Under unsaturated conditions, microorganisms exhibited heightened sensitivity to external disturbances, leading to increased EPS secretion, particularly LB-EPS and polysaccharides, which played a critical role in biofilm formation and microbial adaptation. The secreted EPS curled, resulting in uneven biofilm distribution and reduced bacterial volume. A decrease in saturation inhibited microbial migration, promoted deposition, and reduced interlayer distribution non-uniformity. When saturation dropped to 80 %, further reductions had a diminishing effect on microbial migration. The influence of seepage velocity on microbial breakthrough varied with saturation levels but became negligible at low infiltration rates. Unsaturated conditions weakened the impact of flow rate on microbial breakthrough and deposition, even at higher velocities. Increased flow velocity enhanced bacterial penetration, reduced deposition, and increased deposition non-uniformity. Bioclogging under unsaturated conditions progressed through two stages: (1) the EPS-dominated stage and (2) the EPS-bacterial coaction stage. Enhanced dispersive effects and moisture retention from EPS secretion, combined with reduced flow velocity, significantly influenced bioclogging development. While this study has certain limitations, such as the use of idealized porous media and a limited selection of microbial strains, it nonetheless provides foundational insights into the mechanisms of bioclogging under unsaturated conditions. The results contribute to the theoretical understanding of microbial behavior during stormwater recharge and offer practical implications for the optimization of recharge system design and operation.

CRediT authorship contribution statement

Lyu Tao: Writing – review & editing, Validation, Data curation. **Jia Ruoyu:** Data curation. **Shi Min:** Writing – review & editing, Data curation. **Wang Qiandan:** Formal analysis, Data curation. **Yan Zihan:** Writing – review & editing, Methodology, Formal analysis. **Yang Yuesuo:** Writing – review & editing, Resources, Project administration, Funding acquisition. **Wu Yuhui:** Writing – review & editing, Writing – original draft, Visualization, Methodology, Formal analysis, Data curation, Conceptualization. **Lu Ying:** Writing – review & editing, Validation, Resources, Project administration, Conceptualization. **Chen Jianyu:** Validation. **Song Xiaoming:** Methodology. **Huang Ling:** Writing – review & editing. **Chen Zhiliang:** Funding acquisition.

Declaration of Competing Interest

The authors declare that they have no known competing financial interests or personal relationships that could have appeared to influence the work reported in this paper.

Acknowledgements

This work was supported by the open fund from the Key Lab of Eco-restoration of Regional Contaminated Environment (Shenyang University), Ministry of Education (grant no.: KF-23–10), Special Basic Research Fund for Central Public Research Institutes of China (PM-zx951–202303–125), National Natural Science Foundation of China (42272284, 42277189), China Postdoctoral Science Foundation 2023M732396, Guangxi Key Research and Development Plan (No. Gui ke AB24010113).

Appendix A. Supporting information

Supplementary data associated with this article can be found in the online version at doi:10.1016/j.eti.2025.104228.

Data Availability

The data that has been used is confidential.

References

Abukhanafer, G., Al-Fatlawi, A.H., Joni, H.H., Salman, H.M., 2021. A laboratory investigation to remove the responsible for clogging in filtration process. Environ. Technol. Innov. 21, 101345.

Aramrak, S., Flury, M., Harsh, J.B., Zollars, R.L., 2014. Colloid mobilization and transport during capillary fringe fluctuations. Environ. Sci. Technol. 48 (13), 7272–7279.

Badjana, H.M., Cloke, H.L., Verhoef, A., Julich, S., Camargos, C., Collins, S., Macdonald, D.M.J., McGuire, P.C., Clark, J., 2023. Can hydrological models assess the impact of natural flood management in groundwater-dominated catchments? J. Flood Risk Manag 16 (3), e12912.

Bai, H., Cochet, N., Pauss, A., Lamy, E., 2017. DLVO, hydrophobic, capillary and hydrodynamic forces acting on bacteria at solid-air-water interfaces: Their relative impact on bacteria deposition mechanisms in unsaturated porous media. Colloids Surf. B Biointerfaces 150, 41–49.

Cruz-Paredes, C., Tájmel, D., Rousk, J., 2021. Can moisture affect temperature dependences of microbial growth and respiration? Soil Biol. Biochem 156, 108223.

Cui, G., Liu, Y., Chen, Y.X., Song, T.J., Tong, S.Z., 2021a. Experiments and simulation of co-migration of copper-resistant microorganisms and copper ions in saturated porous media. J. Contam. Hydrol. 242, 103857.

Cui, R.J., Ye, X.Y., Du, X.Q., 2021b. Coupled effects of bacteria and suspended solids on clogging during managed aquifer recharge. J. Hydrol. 600, 126543.

Cui, R.J., Page, D., Du, X.Q., Zhang, H.X., Ye, X.Y., 2023. Effect of iron on biological clogging in porous media: Implications for managed aquifer recharge. Hydrol. Process 37 (3), e14839.

Darnault, C.J.G., Steenhuis, T.S., Garnier, P., Kim, Y.J., Jenkins, M., Ghiorse, W.C., Baveye, P., Parlange, J.Y., 2004. Preferential flow and transport of Cryptosporidium parvum oocysts through the vadose zone: experiments and modeling. Vadose Zone J. 3 (1), 262–270.

Escalante, E.F., 2015. Practical management to minimize the effects of clogging in managed aquifer recharge wells at two sites in the Guadiana Basin, Spain. J. Hydrol. Eng. 20 (3), 1.

Farmer, J., Matthews, R., Smith, P., Langan, C., Hergoualc'h, K., Verchot, L., Smith, J.U., 2014. Comparison of methods for quantifying soil carbon in tropical peats. Geoderma 214 (1), 177–183.

Flemming, H.C., Wingender, J., 2010. The biofilm matrix. Nat. Rev. Microbiol 8 (9), 623–633.

Flury, M., Aramrak, S., 2017. Role of air-water interfaces in colloid transport in porous media: a review. Water Resour. Res. 53 (7), 5247–5275.

Gargiulo, G., Bradford, S.A., Šimůnek, J., Ustohal, P., Vereecken, H., Klumpp, E., 2007. Transport and deposition of metabolically active and stationary phase deinococcus radiodurans in unsaturated porous media. Environ. Sci. Technol. 41 (4), 1265–1271.

Greskowiak, J., Prommer, H., Massmann, G., Johnston, C.D., Nutzmann, G., Pekdeger, A., 2005. The impact of variably saturated conditions on hydrogeochemical changes during artificial recharge of groundwater. Appl. Geochem 20 (7), 1409–1426.

Harimawan, A., Ting, Y.P., 2016. Investigation of extracellular polymeric substances (EPS) properties of P. aeruginosa and B. subtilis and their role in bacterial adhesion. Colloids Surf. B Biointerfaces 146, 459–467.

Hong, P.N., Honda, R., Noguchi, M., Ito, T., 2017. Optimum selection of extraction methods of extracellular polymeric substances in activated sludge for effective extraction of the target components. Biochem. Eng. J. 127, 136–146.

Jara, J., Alarcón, F., Monnappa, A.K., Santos, J.I., Bianco, V., Nie, P., Ciamarra, M.P., Canales, Á., Dinis, L., López-Montero, I., Valeriani, C., Orgaz, B., 2020. Self-adaptation of pseudomonas fluorescens biofilms to hydrodynamic stress. Front. Microbiol 11, 588884.

Jeong, H.Y., Jun, S.C., Cheon, J.Y., Park, M., 2018. A review on clogging mechanisms and managements in aquifer storage and recovery (ASR) applications. Geosci. J. 22 (4), 667–679.

Ke, D., Li, R., Liu, C., 2021. The feedback interaction between biomass accumulation and heterogeneous flow in porous media: Effect of shear stresses. J. Hydrol. 597, 126083.

Lazouskaya, V., Wang, L.P., Gao, H., Shi, X., Czymmek, K., Jin, Y., 2011. Pore-scale investigation of colloid retention and mobilization in the presence of a moving air–water interface. Vadose Zone J. 10 (4), 1250–1260.

Lebon, Y., François, C., Navel, S., Vallier, F., Guillard, L., Pinasseau, L., Oxarango, L., Volatier, L., Mermillod-Blondin, F., 2023. Aquifer recharge by stormwater infiltration basins: hydrological and vadose zone characteristics control the impacts of basins on groundwater chemistry and microbiology. Sci. Total Environ. 865, 161115.

Li, X., Yan, N., Zheng, X.L., Zhao, M.M., Sun, J., Ji, Y.F., 2021. Application of a novel process using biosurfactant rhamnolipid to reduce bioclogging in quartz sand during artificial recharge. J. Hydrol. 595, 126033.

Lin, H.R., Chen, G.C., Long, D.Y., Chen, X.C., 2014. Responses of unsaturated Pseudomonas putida CZ1 biofilms to environmental stresses in relation to the EPS composition and surface morphology. World J. Microbiol. Biotechnol. 30 (12), 3081–3090.

Liu, H., Fang, H.H.P., 2002. Extraction of extracellular polymeric substances (EPS) of sludges. J. Biotechnol. 95 (3), 249–256.

Liu, Y., Tay, J.H., 2002. The essential role of hydrodynamic shear force in the formation of biofilm and granular sludge. Water Res 36 (7), 1653–1665.

Luthy, R.G., Sharvelle, S., Dillon, P., 2019. Urban Stormwater to Enhance Water Supply. Environ. Sci. Technol. 53 (10), 5534–5542.

Manzanera, M., 2021. Dealing with water stress and microbial preservation. Environ. Microbiol 23 (7), 3351–3359.

Marazuela, M.Á., García-Gil, G.A., Santamarta, J.C., Gasco-Cavero, S., Cruz-Pérez, N., Hofmann, T., 2022. Stormwater management in urban areas using dry gallery infiltration systems. Sci. Total Environ. 823, 153705.

Mauclaire, L., Schurmann, A., Thullner, M., Zeyer, J., Gammeter, S., 2004. Sand filtration in a water treatment plant: biological parameters responsible for clogging. In: J. Water Supply Res. Technol, 53. AQUA, pp. 93–108.

Metcalf, E., 2002. Wastewater engineering:treatment and reuse. McGraw-Hill Science Engineering, New York.

Morales, V.L., Parlange, J.Y., Steenhuis, T.S., 2010. Are preferential flow paths perpetuated by microbial activity in the soil matrix? A review. J. Hydrol. 393 (1), 29–36.

More, T.T., Yadav, J.S., Yan, S., Tyagi, R.D., Surampalli, R.Y., 2014. Extracellular polymeric substances of bacteria and their potential environmental applications. J. Environ. Manag 144, 1–25.

Moreno, Z., Paster, A., Kamai, T., 2023. A Wetting-Front Model for Vadose Zone Infiltration via Drywells. Water Resour. Res. 59 (1) e2022WR033554.

Or, D., Phutane, S., Dechesne, A., 2007. Extracellular polymeric substances affecting pore-scale hydrologic conditions for bacterial activity in unsaturated soils. Vadose Zone J. 6 (2), 298–305.

Pan, M., Li, H., Han, X., Ma, W., Li, X., Guo, Q., Yang, B., Ding, C., Ma, Y., 2022. Effects of hydrodynamic conditions on the composition, spatiotemporal distribution of different extracellular polymeric substances and the architecture of biofilms. Chemosphere 307, 135965.

Paul, E., Ochoa, J.C., Pechaud, Y., Liu, Y., Liné, A., 2012. Effect of shear stress and growth conditions on detachment and physical properties of biofilms. Water Res 46 (17), 5499–5508.

Pavelic, P., Dillon, P.J., Mucha, M., Nakai, T., Barry, K.E., Bestland, E., 2011. Laboratory assessment of factors affecting soil clogging of soil aquifer treatment systems. Water Res 45 (10), 3153–3163.

Pechaud, Y., Derlon, N., Queinnec, I., Bessiere, Y., Paul, E., 2024. Modelling biofilm development: The importance of considering the link between EPS distribution, detachment mechanisms and physical properties. Water Res 250, 120985.

Ramazanpour Esfahani, A., Batelaan, O., Hutson, J.L., Fallowfield, H.J., 2020. Combined physical, chemical and biological clogging of managed aquifer recharge and the effect of biofilm on virus transport behavior: A column study. J. Water Process Eng. 33, 101115.

Rathay, S.Y., Allen, D.M., Kirste, D., 2018. Response of a fractured bedrock aquifer to recharge from heavy rainfall events. J. Hydrol. 561, 1048–1062.

Roberson, E.B., Firestone, M.K., 1992. Relationship between desiccation and exopolysaccharide production in a soil Pseudomonas sp. Appl. Environ. Microbiol 58 (4), 1284–1291.
Sen, T.K., 2011. Processes in pathogenic biocolloidal contaminants transport in saturated and unsaturated porous media: A Review. Water Air Soil Pollut. 216 (1-4), 239–256.
Shan, Y.P., Liu, L., Liu, Y., Harms, H., Wick, L.Y., 2020. Effects of electrokinetic phenomena on bacterial deposition monitored by quartz crystal microbalance with dissipation monitoring. Environ. Sci. Technol. 54 (21), 14036–14045.
Shen, Y.X., Xiao, K., Liang, P., Ma, Y.W., Huang, X., 2013. Improvement on the modified Lowry method against interference of divalent cations in soluble protein measurement. Appl. Microbiol. Biotechnol. 97 (9), 4167–4178.
Süßmuth, R., Shrestha, P., Andrea Diaz Navarrete, C., Wege, F.F., Achten, C., Hennecke, D., 2024. Impact of different sterilisation techniques on sorption and NER formation of test chemicals in soil. Chemosphere 357, 141915.
Tong, M.P., Long, G.Y., Jiang, X.J., Kim, H.N., 2010. Contribution of Extracellular Polymeric Substances on Representative Gram Negative and Gram Positive Bacterial Deposition in Porous Media. Environ. Sci. Technol. 44 (7), 2393–2399.
Torkzaban, S., Hassanizadeh, S.M., Schijven, J.F., de Bruin, H.A.M., Husman, A., 2006. Virus transport in saturated and unsaturated sand columns. Vadose Zone J. 5 (3), 877–885.
Wang, H., Xin, J., Zheng, X.L., Li, M., Fang, Y.H., Zheng, T.Y., 2020a. Clogging evolution in porous media under the coexistence of suspended particles and bacteria: Insights into the mechanisms and implications for groundwater recharge. J. Hydrol. 582, 124554.
Wang, H., Xin, J., Zheng, X.L., Fang, Y.H., Zhao, M.M., Zheng, T.Y., 2023. Effect of biofilms on the clogging mechanisms of suspended particles in porous media during artificial recharge. J. Hydrol. 619, 129342.
Wang, Q.D., Lu, Y., Yang, Y.S., Wu, Y.H., Xu, Z., Pei, Z.C., 2022. A study of microbial clogging on the variation of seepage characteristics with biofilm growth in porous media. China Environ. Sci. 42 (06), 2771–2778 (in Chinese).
Wang, T.Z., Guo, Z.C., Shen, Y.J., Cui, Z.M., Goodwin, A., 2020b. Accumulation mechanism of biofilm under different water shear forces along the networked pipelines in a drip irrigation system. Sci. Rep. 10 (1), 6960.
Wei, L.L., Li, J.J., Xue, M., Wang, S., Li, Q.Y., Qin, K.N., Jiang, J.Q., Ding, J., Zhao, Q.L., 2019. Adsorption behaviors of Cu2+ , Zn2+ and Cd2+ onto proteins, humic acid, and polysaccharides extracted from sludge EPS: Sorption properties and mechanisms. Bioresour. Technol. 291, 121868.
Xia, L., Zheng, X.L., Shao, H.B., Xin, A., Peng, T., 2014. Influences of environmental factors on bacterial extracellular polymeric substances production in porous media. J. Hydrol. 519, 3153–3162.
Xia, L., Zheng, X.L., Shao, H.B., Xin, J., Sun, Z.Y., Wang, L.Y., 2016. Effects of bacterial cells and two types of extracellular polymers on bioclogging of sand columns. J. Hydrol. 535, 293–300.
Xia, L., Gao, Z.J., Zheng, X.L., Wei, J.C., 2018. Impact of recharge water temperature on bioclogging during managed aquifer recharge: a laboratory study. Hydrogeol. J. 26 (7), 2173–2187.
Xia, L., Gao, Z.J., Xu, H.L., Feng, G.P., 2020. Variations in bacterial community during bioclogging in Managed Aquifer Recharge (MAR): A laboratory study. Int. Biodeterior. Biodegrad 147, 104843.
Xu, H., Shi, L., Xu, J.Y., Zhang, Z., Yang, X.L., Song, H.L., 2022. Laboratory assessment of media clogging in bioretention systems: Effects of sawdust addition, plant species and dry-wet alternation. J. Water Process Eng. 47, 102764.
Yang, Y.S., Wu, Y.H., Lu, Y., Shi, M., Chen, W.F., 2021. Microorganisms and their metabolic activities affect seepage through porous media in groundwater artificial recharge systems: A review. J. Hydrol. 598, 126256.
Ye, F.X., Ye, Y.F., Li, Y., 2011. Effect of C/N ratio on extracellular polymeric substances (EPS) and physicochemical properties of activated sludge flocs. J. Hazard. Mater. 188 (1), 37–43.
Ye, X.Y., Ma, X.F., Du, X.Q., Cui, R.J., Wan, Y.Y., 2022. Prediction and quantification of bioclogging depth limit and rate based on numerical simulation and experimental validation in managed aquifer recharge. Hydrol. Process 36 (12), 14728.
Zhao, W.Q., Yang, S.S., Huang, Q.Y., Cai, P., 2015. Bacterial cell surface properties: Role of loosely bound extracellular polymeric substances (LB-EPS). Colloids Surf. B Biointerfaces 128, 600–607.
Zheng, X.L., Shan, B.B., Chen, L., Sun, Y.W., Zhang, S.H., 2014. Attachment–detachment dynamics of suspended particle in porous media: Experiment and modeling. J. Hydrol. 511 199–204.

Nature-based stormwater management for aquifer recharge: exploring bioclogging-induced challenges

Wu, Yuhui

2025-08-01

Wu Y, Lu Y, Yan Z, et al., (2025) Nature-based stormwater management for aquifer recharge: exploring bioclogging-induced challenges. Environmental Technology & Innovation, Volume 39, August 2025, Article number 104228

https://doi.org/10.1016/j.eti.2025.104228